REPORT DOCUMENTATION PAGE

Form Approved OMB NO. 0704-0188

1. REPORT DATE (DD-MM-YYYY)	2. REPORT TYPE	3. DATES COVERED (From - To)
	New Reprint	-

4. TITLE AND SUBTITLE
Antibacterial activity of zinc oxide-coated nanoporous alumina

5a. CONTRACT NUMBER
W911NF-10-1-0519

5b. GRANT NUMBER

5c. PROGRAM ELEMENT NUMBER
611102

6. AUTHORS
M.R. Bayati, P.E. Petrochenko, S. Stafslien, J. Daniels, N. Cilz, D.J. Comstock, J.W. Elam, R.J. Narayan, S.A. Skoog

5d. PROJECT NUMBER

5e. TASK NUMBER

5f. WORK UNIT NUMBER

7. PERFORMING ORGANIZATION NAMES AND ADDRESSES
North Dakota State University
111 Dolve Hall
NDSU Dept 2490, PO Box 6050
Fargo, ND 58108 -6050

8. PERFORMING ORGANIZATION REPORT NUMBER

9. SPONSORING/MONITORING AGENCY NAME(S) AND ADDRESS(ES)
U.S. Army Research Office
P.O. Box 12211
Research Triangle Park, NC 27709-2211

10. SPONSOR/MONITOR'S ACRONYM(S)
ARO

11. SPONSOR/MONITOR'S REPORT NUMBER(S)
58401-CH.1

12. DISTRIBUTION AVAILIBILITY STATEMENT
Approved for public release; distribution is unlimited.

13. SUPPLEMENTARY NOTES
The views, opinions and/or findings contained in this report are those of the author(s) and should not contrued as an official Department of the Army position, policy or decision, unless so designated by other documentation.

14. ABSTRACT
Nanoporous alumina membranes, also known as anodized aluminum oxide membranes, are being investigated for use in treatment of burn injuries and other skin wounds. In this study, atomic layer deposition was used for coating the surfaces of nanoporous alumina membranes with zinc oxide. Agar diffusion assays were used to show activity of zinc oxide-coated nanoporous alumina membranes against several bacteria found on the skin surface, including Bacillus subtilis, Escherichia coli, Staphylococcus aureus, and Staphylococcus epidermidis. On the other hand, zinc

15. SUBJECT TERMS
Aluminum oxide, Zinc oxide, Atomic layer deposition, Nanoporous material, Antibacterial material

16. SECURITY CLASSIFICATION OF:			17. LIMITATION OF ABSTRACT	15. NUMBER OF PAGES	19a. NAME OF RESPONSIBLE PERSON
a. REPORT	b. ABSTRACT	c. THIS PAGE			Bret Chisholm
UU	UU	UU	UU		19b. TELEPHONE NUMBER: 701-231-5328

Report Title

Antibacterial activity of zinc oxide-coated nanoporous alumina

ABSTRACT

Nanoporous alumina membranes, also known as anodized aluminum oxide membranes, are being investigated for use in treatment of burn injuries and other skin wounds. In this study, atomic layer deposition was used for coating the surfaces of nanoporous alumina membranes with zinc oxide. Agar diffusion assays were used to show activity of zinc oxide-coated nanoporous alumina membranes against several bacteria found on the skin surface, including Bacillus subtilis, Escherichia coli, Staphylococcus aureus, and Staphylococcus epidermidis. On the other hand, zinc oxide-coated nanoporous alumina membranes did not show activity against Pseudomonas aeruginosa, Enterococcus faecalis, and Candida albicans. These results suggest that zinc oxide-coated nanoporous alumina membranes have activity against some Gram-positive and Gram-negative bacteria that are associated with skin colonization and skin infection.

REPORT DOCUMENTATION PAGE (SF298)
(Continuation Sheet)

Continuation for Block 13

ARO Report Number 58401.1-CH
Antibacterial activity of zinc oxide-coated nanopo ...

Block 13: Supplementary Note

Approved for public release; distribution is unlimited.

Materials Science and Engineering B 177 (2012) 992–998

Contents lists available at SciVerse ScienceDirect

Materials Science and Engineering B

journal homepage: www.elsevier.com/locate/mseb

Short communication

Antibacterial activity of zinc oxide-coated nanoporous alumina

S.A. Skoog[a], M.R. Bayati[b], P.E. Petrochenko[a,c], S. Stafslien[d], J. Daniels[d], N. Cilz[d], D.J. Comstock[e], J.W. Elam[e], R.J. Narayan[a,b,*]

[a] Joint Department of Biomedical Engineering, University of North Carolina and North Carolina State University, Box 7115, Raleigh, NC 27695-7115, USA
[b] Department of Materials Science and Engineering, North Carolina State University, Box 7907, Raleigh, NC 27695-7907, USA
[c] Division of Biology, Office of Science and Engineering Laboratories, Center for Devices and Radiological Health, U.S. Food and Drug Administration, Silver Spring, MD 20993, USA
[d] Center for Nanoscale Science and Engineering, North Dakota State University, 1805 Research Park Drive, Fargo, ND 58102, USA
[e] Energy Systems Division, Argonne National Laboratory, Argonne, IL 60439, USA

ARTICLE INFO

Article history:
Received 21 November 2011
Received in revised form 23 April 2012
Accepted 23 April 2012
Available online 17 May 2012

Keywords:
Aluminum oxide
Zinc oxide
Atomic layer deposition
Nanoporous material
Antibacterial material

ABSTRACT

Nanoporous alumina membranes, also known as anodized aluminum oxide membranes, are being investigated for use in treatment of burn injuries and other skin wounds. In this study, atomic layer deposition was used for coating the surfaces of nanoporous alumina membranes with zinc oxide. Agar diffusion assays were used to show activity of zinc oxide-coated nanoporous alumina membranes against several bacteria found on the skin surface, including *Bacillus subtilis*, *Escherichia coli*, *Staphylococcus aureus*, and *Staphylococcus epidermidis*. On the other hand, zinc oxide-coated nanoporous alumina membranes did not show activity against *Pseudomonas aeruginosa*, *Enterococcus faecalis*, and *Candida albicans*. These results suggest that zinc oxide-coated nanoporous alumina membranes have activity against some Gram-positive and Gram-negative bacteria that are associated with skin colonization and skin infection.

1. Introduction

Several researchers have recently investigated the use of nanostructured membranes for enhanced treatment of wounds [1–3]. For example, Wang et al. described the use of a nanostructured membrane containing N-isopropylacrylamide, methyl methacrylate, and 2-hydroxyethyl methacrylate for wound dressings and cell grafting materials [2]. No cytotoxicity was noted during in vitro studies; growth of cells, including L929 murine neoplastic fibroblasts, and primary human dermal fibroblasts, on these materials was demonstrated. Ceramic membranes may be preferred over polymeric membranes for use in wound treatment applications due to better reproducibility, better control over pore dimensions, an absence of toxic organic solvents, and an absence of toxic polymer degradation byproducts [3]. In recent work, Parkinson et al. examined the use of custom-made nanoporous alumina membranes, which were created by means of anodic oxidation of aluminum in an oxalic acid electrolyte, for treatment of skin wounds and burn injuries [3]. They noted several advantages of nanoporous alumina membranes for wound healing applications, particularly the highly regular structure, biocompatibility, low production cost, reproducible reproduction, and facile reproduction approach for these materials. Using in vitro studies, keratinocytes (HaCaT cell line) and fibroblasts (NIH-3T3) were shown to readily adhere to nanoporous aluminum oxide membranes. In addition, they performed an in vivo study involving application of a nanoporous alumina membrane to a dorsal flank burn injury in a porcine model; the nanoporous alumina membrane adhered to the skin and conformed to the skin. Removal of the membrane from the injury site was not associated with loss of epidermis or inhibition of wound healing. Naji and Harmand demonstrated that amorphous alumina exhibited cytocompatibility using in vitro assays that involved human differentiated alveolar bone osteoblast and gingival fibroblast cultures [4].

Atomic layer deposition may be used to deposit antimicrobial zinc oxide coatings on the surfaces of nanoporous alumina membranes. This technique involves self-terminating chemical reactions between gaseous precursors on the membrane surface, which enable layer-by-layer growth of material [5]. Purge steps, which involve flushing with an inert gas, are performed between gas–solid reactions. If the substrate is saturated during each reaction, then conformal coatings may be deposited on nanoporous materials [6]. Due to these unique capabilities, atomic layer deposition has previously been used to alter pore dimensions and pore surface features in nanoporous materials [7–10]. For example, Moon et al. deposited aluminum oxide

* Corresponding author at: Joint Department of Biomedical Engineering, University of North Carolina and North Carolina State University, Raleigh, NC 27695-7115, USA. Tel.: +1 919 696 8488; fax: +1 919 513 3814.
E-mail address: roger_narayan@msn.com (R.J. Narayan).

0921-5107/$ – see front matter © 2012 Elsevier B.V. All rights reserved.
http://dx.doi.org/10.1016/j.mseb.2012.04.024

within the pores of nanoporous alumina membranes by means of atomic layer deposition, reducing the pore diameter from 70 nm to below 40 nm [11]. Fluorescence microscopy was used to demonstrate selective filtration of bacteriophage phi29 virus nanoparticles using these atomic layer deposition-modified membranes; empty capsids passed through 40 nm diameter pores. On the other hand, most of the DNA-containing capsids remained on the membrane surfaces. Velleman et al. deposited silica coatings on commercially obtained nanoporous alumina membranes; they subsequently modified these silica-coated membranes with perfluorodecyldimethylchlorosilane [12]. These hydrophobic perfluorodecyldimethylchlorosilane/silica-coated nanoporous alumina membranes demonstrated enhanced transport of a hydrophobic agent, tris(2,2′-bipyridyl)dichlororuthenium(II) hexahydrate, over a hydrophilic agent, Rose Bengal.

In several studies over the past two decades, zinc oxide has been shown to possess activity against a broad spectrum of Gram positive and Gram negative bacteria [13,14]. For example, Atmaca et al. showed that zinc exhibited antibacterial activity against *Pseudomonas aeruginosa*, *Staphylococcus aureus*, and *Staphylococcus epidermidis*; their work indicated that zinc-microbial membrane interactions resulted in prolongation of the growth cycle lag phase [15].

Sawai et al. attributed the antimicrobial activity of zinc oxide powder slurry to the release of hydrogen peroxide; results from an in vitro study involving *Escherichia coli* suggested that hydrogen peroxide crosses the microbial cell membrane, resulting in growth inhibition or death [16]. In subsequent work, Sawai et al. showed efficacy by zinc oxide against *S. aureus*, which was attributed to strong affinity between zinc oxide and *S. aureus* cells [17]. Zhang et al. showed that zinc oxide exhibits bacteriostatic activity against *E. coli*; scanning electron microscopy data suggested that zinc oxide-bacteria direct interactions may cause damage and breakdown of bacterial cell membranes [18]. Jones et al. demonstrated activity of zinc oxide nanoparticles against several microorganisms, including *Bacillus subtilis*, *Enterococcus faecalis*, *E. coli*, methicillin-sensitive *S. aureus*, methicillin-resistant *S. aureus*, *S. epidermidis*, and *Streptococcus pyogenes*; they noted that zinc oxide is toxic at high concentrations but is not expected to be toxic at very low concentrations [14]. On the other hand, Xie et al. showed that relatively low concentrations of zinc oxide nanoparticles provided bactericidal activity against *Campylobacter jejuni*; the bactericidal activity was attributed to oxidative stress and cell membrane disruption [19]. Reverse transcription-quantitative polymerase chain reaction studies showed increased expression of two oxidative stress genes and a general stress response gene in zinc oxide nanoparticle-exposed cells. Huang et al. noted damage and disorganization of membranes in *Streptococcus agalactiae* and *S. aureus* after interaction with zinc oxide; this process was attributed to alterations in membrane permeability [20]. Liu et al. showed that zinc oxide inhibited growth of *E. coli* O157:H7; their work indicated the zinc oxide distorted and damaged the cell membrane, which led to release of intracellular material and cell death [21]. It is important to note that zinc oxide exhibits better stability as well as a better safety profile than conventional antimicrobial pharmacologic agents [17].

Several investigators, including Elam et al. and Grigoras et al., have shown that uniform zinc oxide coatings may be grown on nanoporous alumina membranes using atomic layer deposition [22,23]. For example, Sirvio et al. demonstrated conformal growth of zinc oxide coatings on commercially obtained nanoporous alumina membranes (Anodisc®) [24]. More recently, Wang et al. deposited zinc oxide on the surfaces of mesoporous polystyrene-b-poly(2-vinylpyridine) block copolymer nanorods; these nanorods were formed by self-assembly within the pores of nanoporous alumina membranes [25]. Zinc oxide films with low thickness values may grown by means of atomic layer deposition, minimizing concerns associated with dose-dependent toxicity. For example, we previously demonstrated deposition of zinc oxide coatings on 20 nm pore size and 100 nm pore size nanoporous alumina membranes by means of atomic layer deposition [7,8]. In these studies, zinc oxide-coated nanoporous alumina membranes were associated with significantly ($p < 0.05$) higher viability of human epidermal keratinocytes than uncoated nanoporous alumina membranes. In addition, the antimicrobial performance of the zinc oxide-coated nanoporous alumina membranes against two microorganisms was evaluated using agar diffusion assays. In these studies, activity of zinc oxide-coated membranes against *E. coli* and *S. aureus* under continuous tungsten-halogen light exposure and in darkness was demonstrated.

In this study, the surfaces of commercially obtained 20 nm pore size nanoporous alumina membranes and 100 nm pore size nanoporous alumina membranes were coated with zinc oxide using atomic layer deposition. The antimicrobial activity of these zinc oxide-coated nanoporous alumina membranes was evaluated using several microorganisms found on the surface of the skin, including *B. subtilis* [26] (a Gram-positive bacterium), *Candida albicans* [27] (a fungus), *E. faecalis* [28] (a Gram-positive bacterium), *E. coli* [29] (a Gram-negative bacterium), *P. aeruginosa* [30] (a Gram-negative bacterium), *S. aureus* [31] (a Gram-positive bacterium), and *S. epidermidis* [32] (a Gram-positive bacterium). In addition, leaching of zinc from the zinc oxide-coated nanoporous alumina membranes was examined using inductively coupled plasma mass spectrometry.

Membranes with two nanoscale pore sizes, 20 nm pore size nanoporous alumina membranes and 100 nm pore size nanoporous alumina membranes, were obtained from a commercial source (Whatman, Maidstone, United Kingdom); these membranes exhibited thicknesses of 60 μm and outside diameters of 13 mm. The 20 nm pore size nanoporous alumina membranes exhibited pore diameters of 200 nm for ~58 μm of the thickness; the pore diameters tapered to 20 nm for ~2 μm of the thickness. The 100 nm pore size nanoporous alumina membranes exhibited pore diameters of 200 nm for ~58 μm of the thickness; the pore diameters tapered to 100 nm for ~2 μm of the thickness.

Prior to deposition of the zinc oxide coating, the nanoporous alumina membranes were cleaned in situ using flowing ozone. Samples were exposed for 5 min to an ozone partial pressure of ~0.1 Torr; ozone was obtained from ultra high purity oxygen (flow rate = 400 sccm). Zinc oxide coatings were grown using alternating exposure to water and diethyl zinc (Sigma–Aldrich, St. Louis, MO) at a deposition temperature of 200 °C. A precursor exposure time of 6 s, a purge period of 5 s, and a precursor partial pressure of ~0.2 Torr were utilized. A deposition rate ~1.5 A/cycle and a zinc oxide coating thickness of 8 nm were obtained from ellipsometry on Si (1 0 0) witness samples, which were coated at the same time as the nanoporous alumina membranes.

Imaging of the zinc oxide-coated nanoporous alumina membranes was performed using a JEOL 6400 scanning electron microscope (JEOL, Tokyo, Japan) with a field emission source; this instrument was equipped with an energy dispersive X-ray spectrometer attachment. Phase structure for the zinc oxide-coated nanoporous alumina membranes was obtained with a Smartlab X-ray diffraction instrument (Rigaku, The Woodlands, TX) using Cu Kα radiation ($\lambda = 1.54$ nm). Measurements were obtained using a scanning step of 0.05° and dwell time of 2 s per step.

Inductively coupled plasma mass spectrometry was used to evaluate leaching of zinc from the membrane surface. GIBCO® Dulbecco's Modified Eagle Media (DMEM) with L-glutamine (Invitrogen, Carlsbad, CA) was used as a simulated body fluid [33]. Media was supplemented with HyClone fetal bovine serum (Thermo Scientific, Rockford, IL). The final concentration of fetal bovine serum

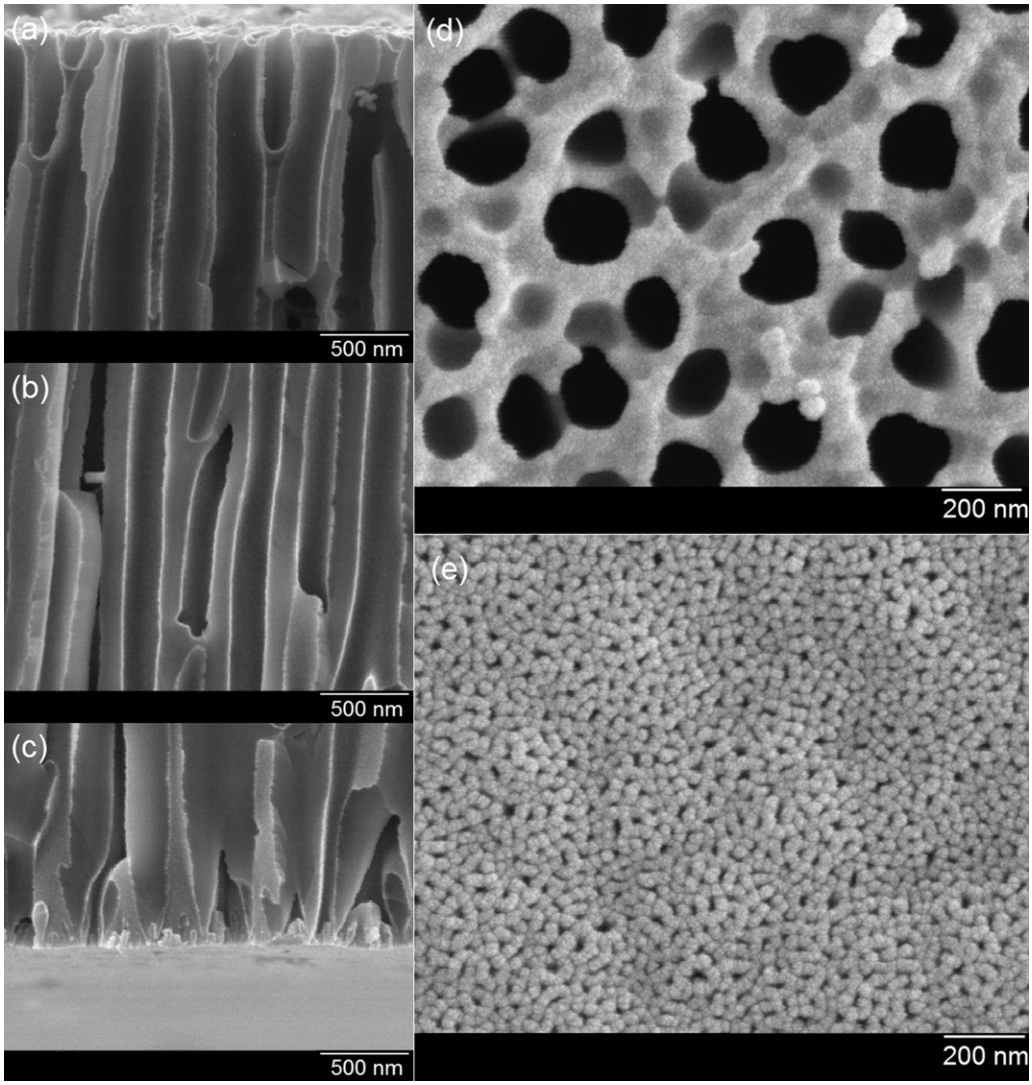

Fig. 1. Scanning electron microscopy images obtained from a 20 nm pore size nanoporous alumina membrane following deposition of an eight nanometer-thick zinc oxide coating. Micrographs obtained from (a) the large pore side, (b) the middle of the pore, and (c) the small pore side of a cleaved specimen show a continuous zinc oxide coating. Plan-view scanning electron micrographs obtained from (d) the large pore side of the membrane and (e) the small pore side of the membrane also show a continuous zinc oxide coating.

in the media was 10%. Membranes were completely immersed in 1 mL of fluid and incubated at 37 °C in an atmosphere containing 5% CO_2 to better simulate an in vivo environment. A total of 12 different membranes, 3 zinc oxide-coated membranes and 3 uncoated membranes for both 20 nm and 100 nm pore sizes, were used to collect extracts. Three wells that contained media but did not contain membranes served as control extracts. A Model 820 inductively coupled plasma mass spectrometer (Varian, Salt Lake City, UT) was used for all elemental analysis measurements. The source has a MicroMist nebulizer (maximum flow rate = 0.4 mL/min), which was used for sample introduction into the plasma. Standard plasma conditions (power = 1.4 kW, plasma flow = 18.00 L/min, auxiliary flow = 1.80 L/min, sheath gas flow = 0.18 L/min, sampling depth = 7.5 mm) were used in this study. All of the solutions were prepared using 18 MΩ de-ionized water (lab supply) and trace metal grade nitric acid (Thermo Fisher Scientific, Waltham, NA). Instrument conditions were optimized using the auto-optimization feature of the instrument. Samples were introduced while peristaltic pump was operated at 3 rpm. The spray chamber was cooled to 3 °C. Standards were prepared using inductively coupled plasma standards that were purchased from a commercial source (Inorganic Ventures, Christiansburg, VA). In all of the measurements, a 5 ppb solution of indium was used as an internal standard and mixed online with each sample through a tee. Isotopes (e.g., ^{66}Zn and ^{115}In) were evaluated in a peak hopping mode; a dwell time of 50,000 μs was used and five replicates of an average of twenty data points were measured. The standard curve included at least eight concentration levels in the quantification range. The standard data set was fitted to a linear curve. The coefficient of correlation was 0.99. Percent errors in calculated concentrations were 15% or lower.

Microbial growth on zinc oxide-coated nanoporous alumina membranes and uncoated nanoporous alumina membranes was determined using the agar plating method. The agar diffusion assay protocol used in this study is similar to one that is outlined by the National Committee for Clinical Laboratory Standards. This approach is appropriate for assessing growth of common microorganisms, including rapidly growing microorganisms [34]. The agar diffusion assay protocol provides qualitative data regarding the susceptibility of a given microorganism to an antimicrobial agent. Tryptic soy broth, Luria–Bertani broth, brain heart infusion broth, Mueller Hinton agar, yeast nitrogen base, dextrose, agar and phosphate-buffered saline (10×) were obtained from a commercial source (VWR International, West Chester, PA). Phosphate-buffered

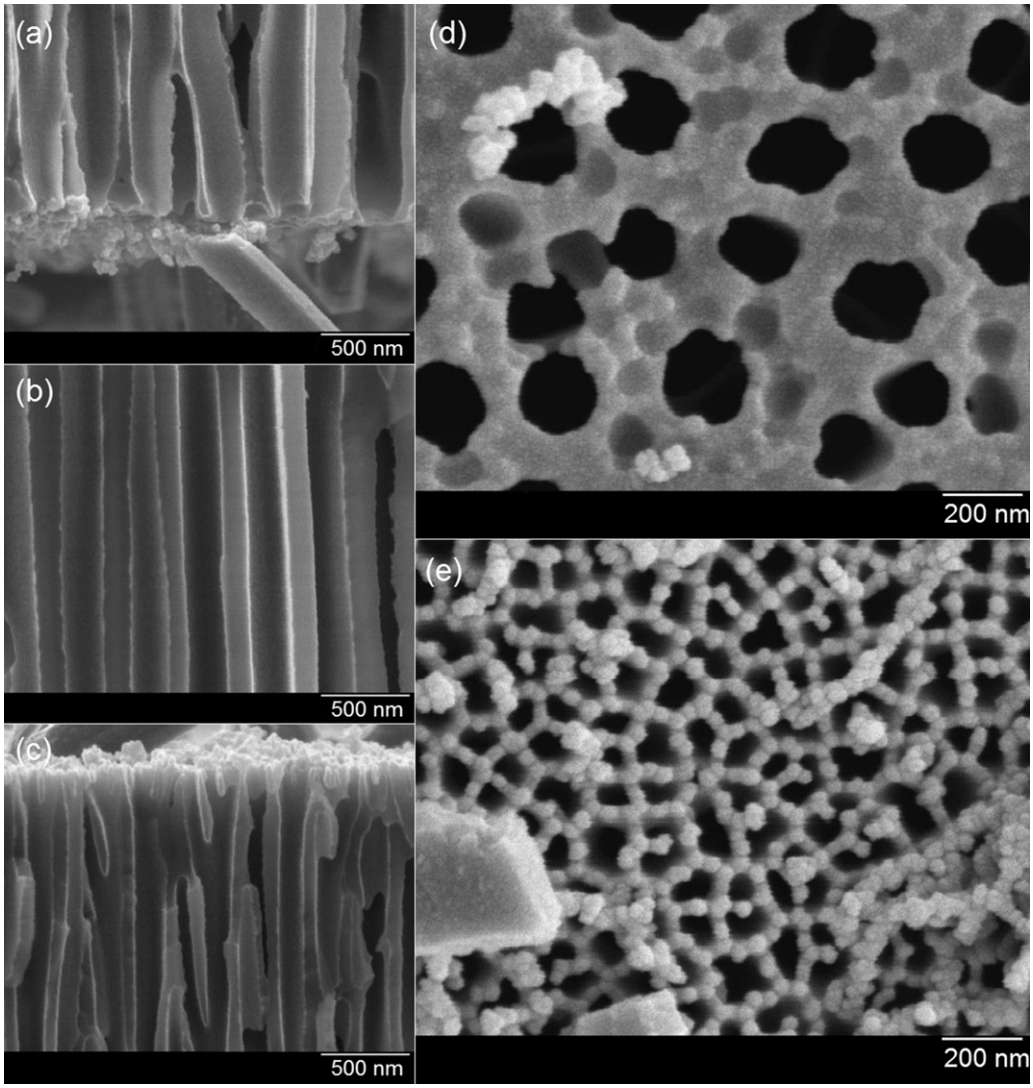

Fig. 2. Scanning electron microscopy images obtained from a 100 nm pore size nanoporous alumina membrane following deposition of an eight nanometer-thick zinc oxide coating. Micrographs obtained from (a) the large pore side, (b) the middle of the pore, and (c) the small pore side of a cleaved specimen show a continuous zinc oxide coating. Plan-view scanning electron micrographs obtained from (d) the large pore side of the membrane and (e) the small pore side of the membrane also show a continuous zinc oxide coating.

saline (1×) was prepared in deionized water. Cultures of *E. coli* ATCC 12435, *E. faecalis* ATCC 29212, *B. subtilis* ATCC 6051, *P. aeruginosa* ATCC 15442, *S. aureus* ATCC 6538, and *S. epidermidis* ATCC 35984 were obtained from a commercial source (American Type Culture Collection, Manassas, VA). Overnight cultures of *E. coli* in Luria–Bertani broth, *E. faecalis* in brain heart infusion broth, *B. subtilis* in tryptic soy broth, *P. aeruginosa* in tryptic soy broth, *S. epidermidis* in tryptic soy broth, *S. aureus* in tryptic soy broth, and *C. albicans* in yeast nitrogen base + 100 mM dextrose were pelleted via centrifugation (4500 rpm) for 10 min. These solutions were subsequently resuspended in phosphate-buffered saline (1×) in order to obtain a final cell density of approximately 10^8 cells/mL. Sterile swabs were used to inoculate lawns of the bacterial strains on Mueller Hinton agar plates and to inoculate lawns of *C. albicans* on yeast nitrogen base + dextrose plates. Zinc oxide-coated nanoporous alumina membranes and uncoated nanoporous alumina membranes were then placed on the inoculated agar plates. The plates were incubated for 24 h at 37 °C. Zones of growth inhibition were visually evaluated from digital images, which were obtained after 24 h of incubation. Growth inhibition on the agar in direct contact with the membrane surfaces was evaluated by removing each membrane and visually inspecting the agar.

Figs. 1 and 2 show scanning electron microscopy images obtained from a 20 nm pore size nanoporous alumina membrane and a 100 nm pore size nanoporous alumina membrane following deposition of an eight nanometer-thick zinc oxide coating, respectively. Plan-view scanning electron micrographs of the large pore sides (Figs. 1(d) and 2(d)) and the small pore sides (Figs. 1(e) and 2(e)) of the zinc oxide-coated nanoporous alumina membranes show that these materials exhibited monodisperse pore sizes and high porosities. Images of the pores within the zinc oxide-coated nanoporous alumina membranes were acquired from cleaved specimens (Figs. 1(a)–(c) and 2(a)–(c)). Images obtained from the large pore side, the middle of the pore, and the small pore side of the cleaved 20 nm pore size nanoporous alumina membrane and the cleaved 100 nm pore size nanoporous alumina membrane show continuous coatings of zinc oxide nanocrystals. These images also indicate that the pore dimensions are not completely uniform; some pore branching was observed. Branching of the pores has been previously noted in the as-received membrane [35,36].

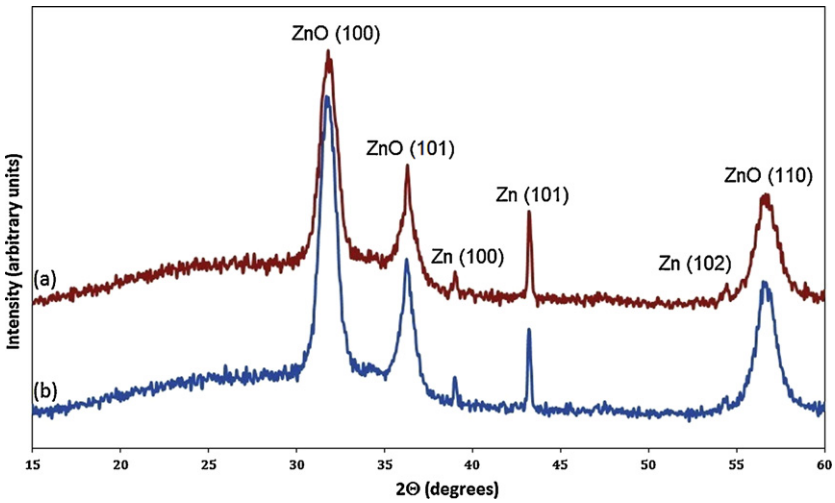

Fig. 3. X-ray diffraction patterns for zinc oxide-coated nanoporous alumina membranes. Pattern (a) shown as a red line, corresponds to data from a 100 nm pore size nanoporous alumina membrane following deposition of an eight nanometer-thick zinc oxide coating. Pattern (b) shown as a blue line, corresponds to data from a 20 nm pore size nanoporous alumina membrane following deposition of an eight nanometer-thick zinc oxide coating. (For interpretation of the references to color in this figure legend and text, the reader is referred to the web version of this article.)

In addition, energy dispersive X-ray analysis performed at the large pore side, the middle of the pore, and the small pore side of the cleaved specimens demonstrated the presence of zinc oxide throughout the pore.

Fig. 3 contains X-ray diffraction patterns for zinc oxide-coated nanoporous alumina membranes. Pattern (a), shown as a red line, corresponds to data from a 20 nm pore size nanoporous alumina membrane following deposition of an eight nanometer-thick zinc oxide coating. Pattern (b), shown as a blue line, corresponds to data from a 100 nm pore size nanoporous alumina membrane following deposition of an eight nanometer-thick zinc oxide coating. The sharp peaks in this figure corresponded with the expected positions for polycrystalline zinc oxide and zinc. The peak located at 2θ of 31.66° corresponded with ZnO (1 0 0). The broad peak corresponded with the nanoporous alumina membrane [37]. As noted by Yoshino et al., Fang et al., and Fang et al., the crystallinity of zinc oxide on nanoporous alumina membranes is affected by surface morphology; as such, it is disordered near the zinc oxide/alumina interface [38–40]. The crystalline size was calculated using the Scherer equation ($D = 0.89\lambda/\pi\beta\cos\theta$); in this equation, θ is the diffraction angle, λ is the X-ray wavelength, β is the full width at half maximum (FWHM) of the diffraction peak, and D is the crystal size [41]. The crystalline size of the zinc oxide-coated 100 nm pore size nanoporous alumina membrane and the 20 nm pore size nanoporous alumina membrane were shown to be 3.3 nm and 5.0 nm, respectively. A metallic zinc phase was observed in the zinc coated-nanoporous alumina membranes. Previous work by Libera et al. has indicated that this zinc phase forms through thermal decomposition of excess diethyl zinc at temperatures greater than 150 °C [42]. Formation of this phase is dependent on the presence of excess diethyl zinc and occurs after saturation of atomic layer deposition surface reactions. The broad hump between $\theta = 20°$ and $\theta = 40°$ is attributed to the amorphous structure of the alumina membrane [43].

Both 20 nm and 100 nm membranes released similar amounts of zinc ions or particulates into the surrounding fluid. Extracts from the zinc oxide-coated 20 nm pore size nanoporous alumina membranes and the zinc oxide-coated 100 nm pore size nanoporous alumina membranes contained similar zinc concentrations of 91.3 ± 3.6 and 92.9 ± 4.6 μg/mL, respectively. Trace amounts of zinc were detected in media and in uncoated membrane controls; this result was expected since zinc is an essential element in cell culture medium. Degen and Kosec noted that immersion of zinc oxide in water results in the surface of the oxide being hydrolyzed and a hydroxide layer being formed. This surface hydroxide ($Zn(OH)_2(s)$) is in equilibrium with $Zn^{2+}{}_{(aq)}$, $Zn(OH)^{+}{}_{(aq)}$, and $Zn(OH)_{2(aq)}$ over pH values between 6 and 8 at a temperature of 25 °C [44].

Fig. 4 contains light microscopy images of agar plating assay results after 24 h of incubation for zinc oxide-coated nanoporous alumina membranes and uncoated nanoporous alumina membranes. Agar plating assay results for zinc oxide-coated nanoporous alumina membranes with 20 nm pore sizes and 100 nm pore sizes against a given microorganism were similar; in addition, agar plating assay results for uncoated nanoporous alumina membranes with 20 nm pore sizes and 100 nm pore sizes against a given microorganism were similar. It is clear from these images that the zinc oxide-coated nanoporous alumina membranes were highly effective toward *S. aureus*, *S. epidermidis* and *B. subtilis*; large zones of growth inhibition for all three bacteria were observed. Zones of growth inhibition were not observed for the other tested microorganisms. Inhibition of *E. coli* growth was evident on the agar surface that was in direct contact with the zinc oxide-coated nanoporous alumina membranes. For *P. aeruginosa*, *E. faecalis* and *C. albicans*, microbial growth was observed on agar surface that was in direct contact with the zinc oxide-coated nanoporous alumina membranes. Zones of growth inhibition were not observed for the uncoated nanoporous alumina membranes in all cases. Furthermore, microbial growth was observed on agar surfaces that were in direct contact with the uncoated nanoporous alumina membranes for all of the organisms. These results suggest that the zinc oxide-coated nanoporous alumina membranes are more effective toward Gram-positive bacteria than Gram-negative bacteria; in addition, zinc oxide-coated nanoporous alumina membranes are essentially ineffective toward yeast. Previous work by Sawai et al. also noted that zinc oxide exhibits stronger activity against Gram-positive bacteria than Gram-negative bacteria [45].

The results of this study suggest that zinc oxide-coated nanoporous alumina membranes have activity against some microorganisms that are observed on the surface of the skin. The zinc oxide-coated membranes showed activity against *B. subtilis*, *E. coli*, *S. aureus*, and *S. epidermidis* in agar diffusion assays. On the other hand, the zinc oxide-coated membranes did not show activity against *P. aeruginosa*, *E. faecalis*, and *C. albicans*. There are

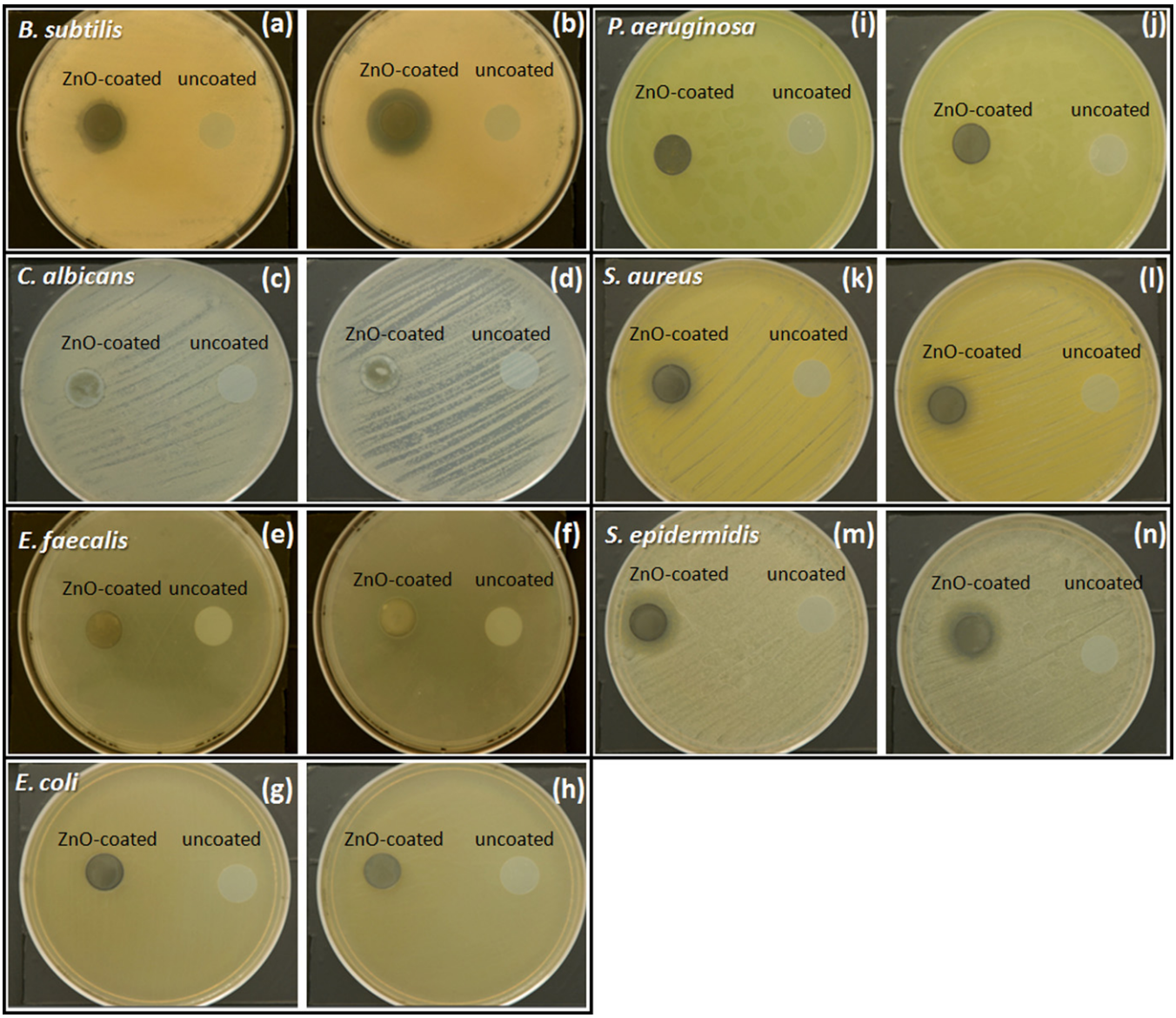

Fig. 4. Light microscopy images of agar plating assay results after 24 h of incubation for zinc oxide-coated nanoporous alumina membranes and uncoated nanoporous alumina membranes. Images (a) and (b) show uncoated and zinc oxide-coated nanoporous alumina membranes with (a) 20 nm pore sizes and (b) 100 nm pore sizes that were examined against *Bacillus subtilis*. Images (c) and (d) show uncoated and zinc oxide-coated nanoporous alumina membranes with (c) 20 nm pore sizes and (d) 100 nm pore sizes that were examined against *Candida albicans*. Images (e) and (f) show uncoated and zinc oxide-coated nanoporous alumina membranes with (e) 20 nm pore sizes and (f) 100 nm pore sizes that were examined against *Enterococcus faecalis*. Images (g) and (h) show uncoated and zinc oxide-coated nanoporous alumina membranes with (g) 20 nm pore sizes and (h) 100 nm pore sizes that were examined against *Escherichia coli*. Images (i) and (j) show uncoated and zinc oxide-coated nanoporous alumina membranes with (i) 20 nm pore sizes and (j) 100 nm pore sizes that were examined against *Pseudomonas aeruginosa*. Images (k) and (l) show uncoated and zinc oxide-coated nanoporous alumina membranes with (k) 20 nm pore sizes and (l) 100 nm pore sizes that were examined against *Staphylococcus aureus*. Images (m) and (n) show uncoated and zinc oxide-coated nanoporous alumina membranes with (m) 20 pore sizes nm and (n) 100 nm pore sizes that were examined against *Staphylococcus epidermidis*.

several potential dermatologic applications for zinc oxide-coated nanoporous alumina membranes, including use in tissue coverage and/or cell transplantation at burn sites [2].

Acknowledgments

SS, JD, and NC would like acknowledge support from Army Research Office Contract Number W911NF-10-1-0519. The submitted manuscript has been created in part by UChicago Argonne, LLC, Operator of Argonne National Laboratory (“Argonne”). Argonne, a U.S. Department of Energy Office of Science laboratory, is operated under Contract No. DE-AC02-06CH11357.

References

[1] B.S. Smith, S. Yoriya, T. Johnson, K.C. Popat, Acta Biomaterialia 7 (2011) 2686–2696.
[2] L.S. Wang, P.Y. Chow, T.T. Phan, I.J. Lim, Y.Y. Yang, Advanced Functional Materials 16 (2006) 1171–1178.
[3] L.G. Parkinson, N.L. Giles, K.F. Adcroft, M.W. Fear, F.M. Wood, G.E. Poinern, Tissue Engineering Part A 15 (2009) 3753–3763.
[4] A. Naji, M.F. Harmand, Biomaterials 12 (1991) 690–694.
[5] G. Xiong, J.W. Elam, H. Feng, C.Y. Han, H.H. Wang, L.E. Iton, L.A. Curtiss, M.J. Pellin, M. Kung, H. Kung, P.C. Stair, Journal of Physical Chemistry B 109 (2005) 14059–14063.
[6] J.J. Wang, X. Deng, R. Varghese, A. Nikolov, P. Sciortino, F. Liu, L. Chen, X. Liu, Journal of Vacuum Science and Technology B 23 (2005) 3209–3213.
[7] R.J. Narayan, S.P. Adiga, M.J. Pellin, L.A. Curtiss, A.J. Hryn, S. Stafslien, B. Chisholm, C.C. Shih, C.M. Shih, S.J. Lin, Y.Y. Su, C. Jin, J. Zhang,

N.A. Monteiro-Riviere, J.W. Elam, Philosophical Transactions of the Royal Society A 368 (2010) 2033–2064.
[8] R.J. Narayan, S.P. Adiga, M.J. Pellin, L.A. Curtiss, S. Stafslien, B. Chisholm, N.A. Monteiro-Riviere, R.L. Brigmon, J.W. Elam, Materials Today 13 (2010) 60–64.
[9] R.J. Narayan, N.A. Monteiro-Riviere, R.L. Brigmon, M.J. Pellin, J.W. Elam, JOM 61 (2009) 12–16.
[10] S.P. Adiga, C. Jin, L.A. Curtiss, N.A. Monteiro-Riviere, R.J. Narayan, Wiley Interdisciplinary Reviews: Nanomedicine and Nanobiotechnology 1 (2009) 568–581.
[11] J.M. Moon, D. Akin, Y. Xuan, P.D. Ye, P. Guo, R. Bashir, Biomedical Microdevices 11 (2009) 135–142.
[12] L. Velleman, G. Triani, P.J. Evans, J.G. Shapter, D. Losic, Microporous and Mesoporous Materials 126 (2009) 87–94.
[13] Q. Li, S. Mahendra, D.Y. Lyon, L. Brunet, M.V. Liga, D. Li, P.J. Alvarez, Water Research 42 (2008) 4591–4602.
[14] N. Jones, B. Ray, K.T. Ranjit, A.C. Manna, FEMS Microbiology Letters 279 (2008) 71–76.
[15] S. Atmaca, K. Gul, R. Clcek, Turkish Journal of Medical Sciences 28 (1998) 595–597.
[16] J. Sawai, S. Shoji, H. Igarashi, A. Hashimoto, T. Kokugan, M. Shimizu, H. Kojima, Journal of Fermentation and Bioengineering 86 (1998) 521–522.
[17] J. Sawai, Journal of Microbiology Methods 54 (2003) 177–182.
[18] L.L. Zhang, Y.H. Jiang, Y.L. Ding, M. Povey, D. York, Journal of Nanoparticle Research 9 (2007) 479–489.
[19] Y.P. Xie, Y.P. He, P.L. Irwin, T. Jin, X.M. Shi, Applied and Environment Microbiology 77 (2011) 2325–2331.
[20] Z. Huang, X. Zheng, D. Yan, G. Yin, X. Liao, Y. Kang, Y. Yao, D. Huang, B. Hao, Langmuir 24 (2008) 4140–4144.
[21] Y. Liu, L. He, A. Mustapha, H. Li, Z.Q. Hu, M. Lin, Journal of Applied Microbiology 107 (2009) 1193–1201.
[22] J.W. Elam, D. Routkevitch, P.P. Mardilovich, S.M. George, Chemistry of Materials 15 (2003) 3507–3517.
[23] K. Grigoras, V.M. Airaksinen, S. Franssila, Journal of Nanoscience and Nanotechnology 9 (2009) 3763–3770.
[24] S. Sirvio, L. Sainiemi, S. Franssila, K. Grigoras, Transducers 2007–2007 International Solid-state Sensors, Actuators and Microsystems Conference 2007 (2007) 521–524.
[25] Y. Wang, Y. Qin, A. Berger, E. Yau, C. He, L. Zhang, U. Goesele, M. Knez, M. Steinhart, Advanced Materials 21 (2009) 2763–2766.
[26] K. Ara, M. Hama, S. Akiba, K. Koike, K. Okisaka, T. Hagura, T. Kamiya, F. Tomita, Canadian Journal of Microbiology 52 (2006) 357–364.
[27] S. Kagami, H.L. Rizzo, S.E. Kurtz, L.S. Miller, A. Blauvelt, Journal of Immunology 185 (2010) 5453–5462.
[28] M.A. Pfaller, P.R. Rhomberg, H.S. Sader, R.E. Mendes, R.N. Jones, Journal of Chemotherapy 22 (2010) 304–311.
[29] P. Mohan, B. Ramu, E. Bhaskar, J. Venkataraman, Annals of Hepatology 10 (2011) 15–20.
[30] G. Eslami, F. Fallah, H. Goudarzi, M. Navidinia, Gene Therapy and Molecular Biology 10B (2006) 263–267.
[31] L.G. Miller, C. Quan, A. Shay, K. Mostafaie, K. Bharadwa, N. Tan, K. Matayoshi, J. Cronin, J. Tan, G. Tagudar, A.S. Bayer, Clinical Infectious Diseases 44 (2007) 483–492.
[32] A. Bashir, T.Y. Mujahid, N. Jehan, Pakistan Journal of Pharmaceutical Sciences 20 (2007) 299–304.
[33] J.T.Y. Lee, Y. Leng, K.L. Chow, F.Z. Ren, X. Ge, K.F. Wang, X. Lu, Acta Biomaterialia 7 (2011) 2615–2622.
[34] M.A. Wikler, J.F. Hindley, F.R. Cockerill, J.B. Patel, K. Bush, M. Powell, M.N. Dudley, J.D. Turnidge, G.M. Eliopoulos, M.P. Weinstein, D.J. Hardy, B.L. Zimmer, D.W. Hecht, M.J. Ferraro, J.M. Swenson, Performance Standards for Antimicrobial Disk Susceptibility Tests, Approved Standard-Tenth Edition M02-A10, Clinical and Laboratory Standards Institute, Wayne, PA, 2009.
[35] P. Kodumuri, In situ growth of porous alumino-silicates and fabrication of nanoporous membranes, PhD thesis, Cleveland State University, 2009.
[36] S. Habouti, C.H. Solterbeck, M. Es-Souni, Journal of Materials Chemistry 20 (2010) 5215–5219.
[37] Z. Wang, H.L. Li, Applied Physics A 74 (2002) 201–203.
[38] Z. Fang, Y. Wang, X. Peng, X. Liu, C. Zhen, Materials Letters 57 (2003) 4187–4190.
[39] Y. Yoshino, K. Inoue, M. Takeuchi, T. Makino, Y. Katayama, T. Hata, Vacuum 59 (2000) 403–410.
[40] Y. Yoshino, K. Inoue, M. Takeuchi, K. Ohwada, Vacuum 51 (1998) 601–607.
[41] A.L. Patterson, Physical Review 56 (1939) 978–982.
[42] J.A. Libera, J.W. Elam, M.J. Pellin, Thin Solid Films 516 (2008) 6158–6166.
[43] H. Zhang, X. Li, G. Hu, Y. Li, Journal of Materials Science Materials in Medicine 21 (2010) 950–953.
[44] A. Degen, M. Kosec, Journal of the European Ceramic Society 20 (2000) 667–673.
[45] J. Sawai, H. Igarashi, A. Hashimoto, T. Kokugan, M. Shimizu, Journal of Chemical Engineering of Japan 28 (1995) 288–293.